

## Supporting Information

for *Laser Photonics Rev.*, DOI 10.1002/lpor.202300346

Revealing Mie Resonances with Enhanced and Suppressed Second-Order Nonlinear Optical Responses in a Hexagonal-Prism-Like MoS<sub>2</sub> Nanoparticle

*Mingcheng Panmai, Jin Xiang, Lidan Zhou, Shulei Li and Sheng Lan\**

Copyright WILEY-VCH Verlag GmbH & Co. KGaA, 69469 Weinheim, Germany, 2018.

## Supporting Information

Revealing Mie resonances with enhanced and suppressed second-order nonlinear optical responses in a hexagonal-prism-like MoS<sub>2</sub> nanoparticle

Mingcheng Panmai, Lidan Zhou, Shulei Li, and Sheng Lan\*

Mr. Mingcheng Panmai, Ms. Lidan Zhou, and Prof. Sheng Lan  
Guangdong Provincial Key Laboratory of Nanophotonic Functional Materials and Devices, School of Information and Optoelectronic Science and Engineering, South China Normal University, Guangzhou 510006, P. R. China  
[slan@scnu.edu.cn](mailto:slan@scnu.edu.cn) (S. Lan)

Ms. Lidan Zhou  
State Key Laboratory of Optoelectronic Materials and Technologies, School of Electronics and Information Technology, Sun Yat-sen University, Guangzhou 51006, P. R. China

Dr. Shulei Li,  
School of Optoelectronic Engineering, Guangdong Polytechnic Normal University, Guangzhou 510665, P. R. China

### Table of contents

1. Morphology characterization of MoS<sub>2</sub> nanoparticles
2. Scattering spectrum and of MoS<sub>2</sub> nanoparticles
3. Dependence of the scattering spectrum on the polarization of the excitation light
4. Dependences of the optical modes on the geometrical parameters
5. CCD images of the SHG
6. Optical mode with suppressed SHG
7. Optical mode with enhanced SHG
8. Emission pattern of the SHG
9. Finding MoS<sub>2</sub> nanoparticles with suppressed SHG by using laser scanning confocal microscope
10. MoS<sub>2</sub> monolayer attached on an ITO substrate
11. Nonlinear optical responses of MoS<sub>2</sub> nanodisks

### Note 1 Morphology characterization of MoS<sub>2</sub> nanoparticles

We selected MoS<sub>2</sub> nanoparticles with regular morphologies from MoS<sub>2</sub> powder purchased from the supplier (Sixcarbon Tech Shenzhen). In Fig. [S1a](#), we show the SEM image of MoS<sub>2</sub> powder. It contains nanoparticles and nanosheets with different shapes and sizes. In Fig. [S1b](#), we present the magnified images of some nanoparticles and nanosheets. It is noticed that a MoS<sub>2</sub> nanoparticle is generally composed of vertically stacked layers, as shown in Fig. [S1c](#) where the side view of a

nanoparticle is presented. In Fig. S1d, we show the SEM image of a hexagonal-prism-like nanoparticle successfully selected from the powder. The AFM image is shown in the inset.

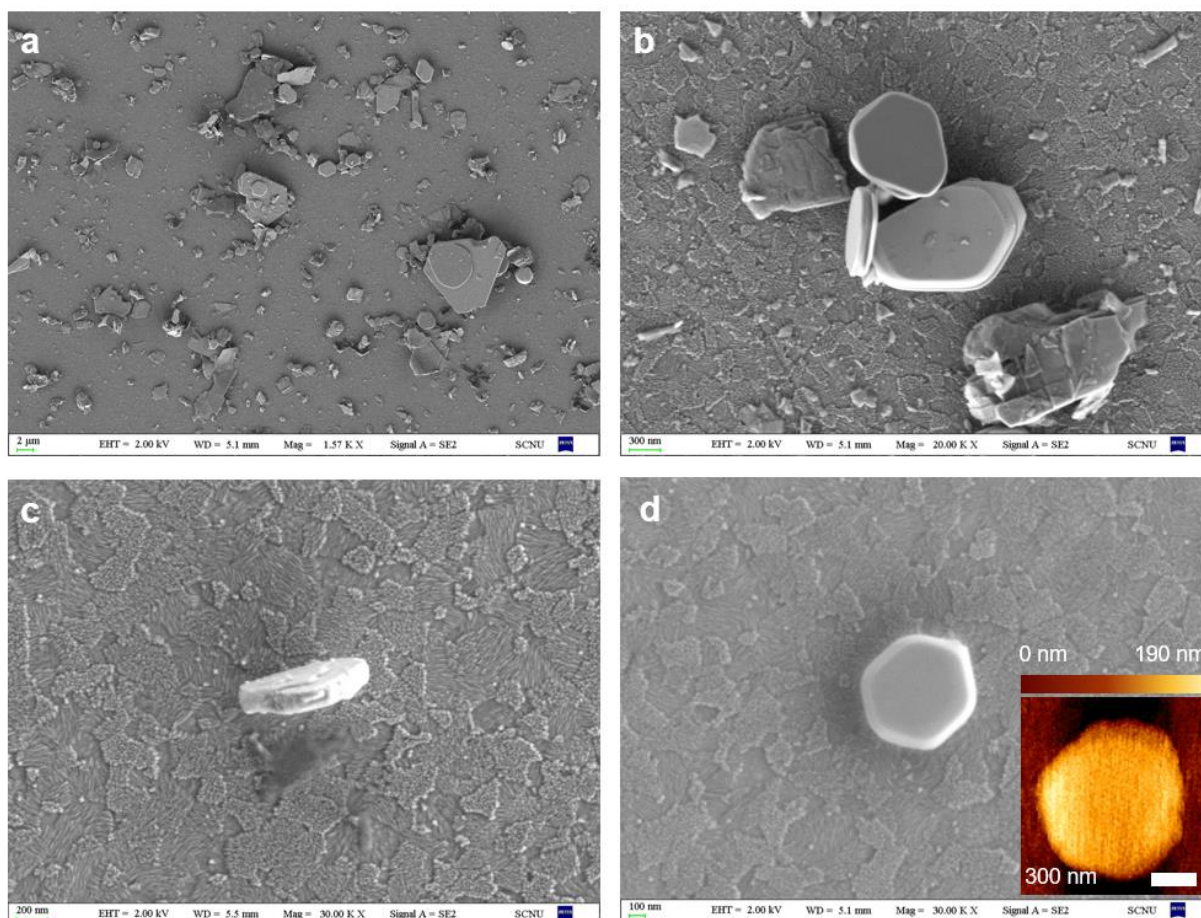


Figure S1 Morphology characterization of MoS<sub>2</sub> nanoparticles. (a) SEM image (top view) of MoS<sub>2</sub> powder distributed on an ITO substrate. (b) Magnified SEM images of MoS<sub>2</sub> nanoparticles and nanosheets. (c) Side view of a MoS<sub>2</sub> nanoparticle. (d) Top view of a hexagonal-prism-like MoS<sub>2</sub> nanoparticle. The AFM image is shown in the inset.

#### Note 2 Scattering spectra of MoS<sub>2</sub> nanoparticles

In Fig. S2, we show the scattering spectra measured for three MoS<sub>2</sub> nanoparticles. The scattering dips originating from the absorption of excitons are clearly identified at ~660 and ~610 nm.

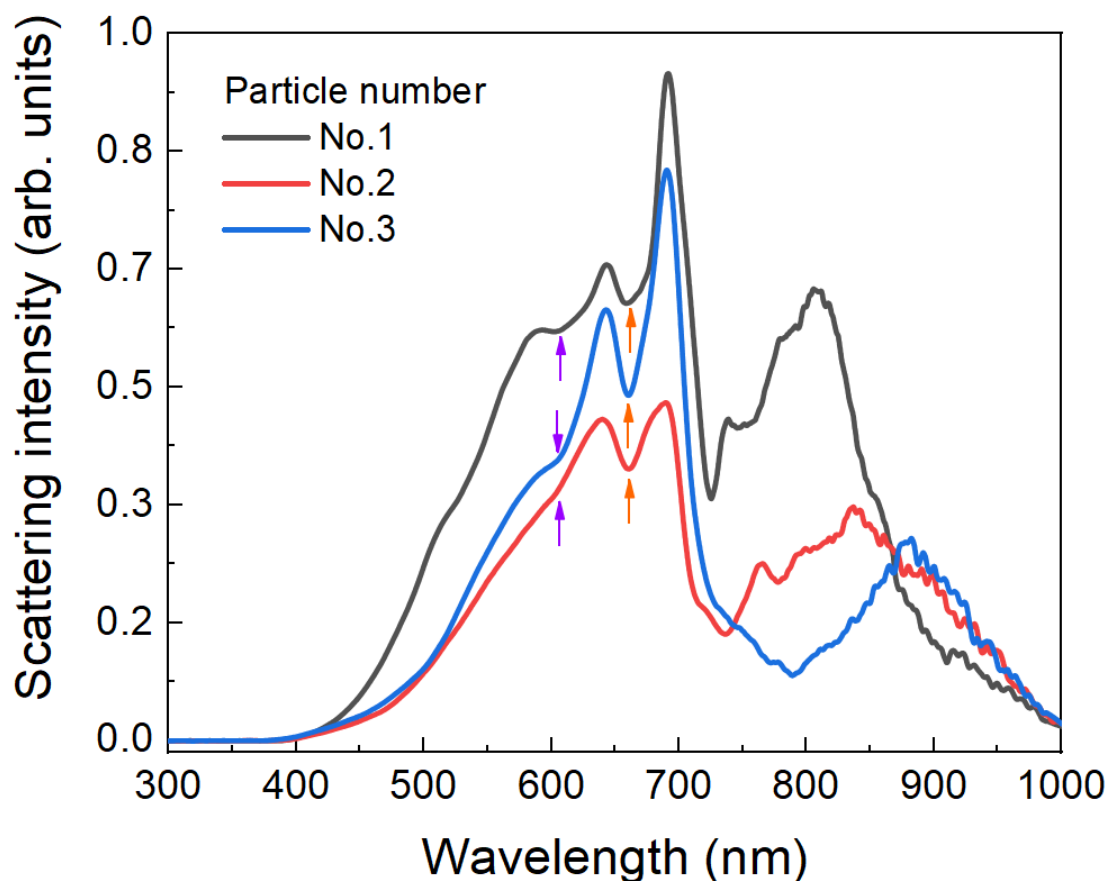


Figure S2 Scattering spectra measured for three MoS<sub>2</sub> nanoparticles with different geometrical parameters. The two exciton resonances appearing as scattering dips are marked by arrows.

Note 3 Dependence of the scattering spectrum on the polarization of the excitation light

We simulated the scattering spectra of a typical MoS<sub>2</sub> nanoparticle with  $l = 300$  nm and  $h = 170$  nm, which is excited by using white light polarized along the arm chair and zigzag directions. As shown in Figs. S3a and S3b, the scattering spectrum of the MoS<sub>2</sub> nanoparticle depends weakly on the polarization of the excitation light.

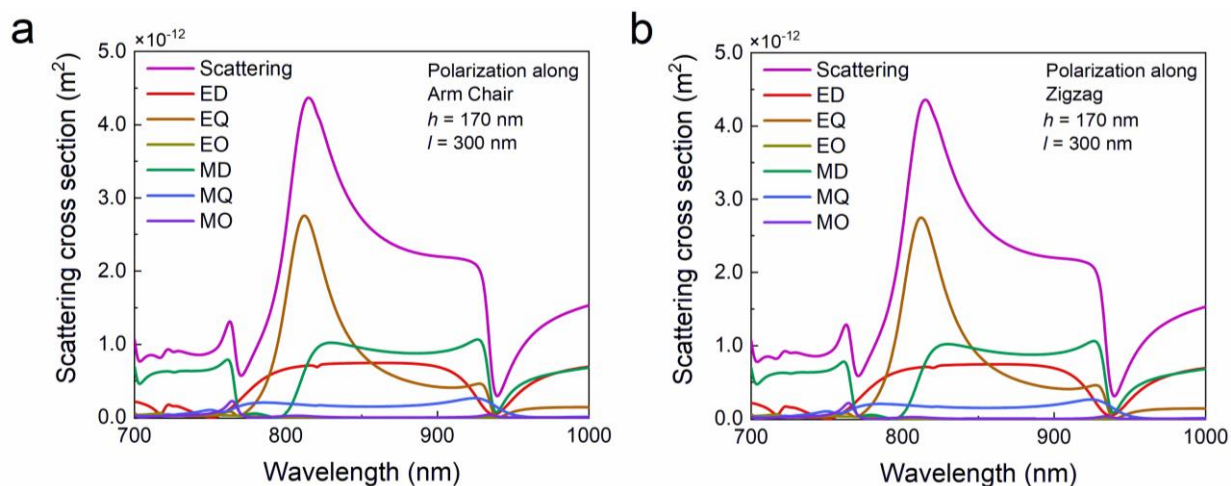


Figure S3 Scattering spectra calculated for a MoS<sub>2</sub> nanoparticles with  $l = 300$  nm and  $h = 170$  nm excited by using white light polarized along the arm chair direction (a) and the zigzag direction (b).

## Note 4 Dependences of the optical modes on the geometrical parameters

The thickness of a MoS<sub>2</sub> nanoparticle was characterized by using atomic force microscopy (AFM). The errors in the AFM measurements can be evaluated by the simulation results. In Fig. S4a, we show the scattering spectra of MoS<sub>2</sub> nanoparticles with the same length ( $l = 300$  nm) and different heights ( $h = 130$ – $210$  nm). Thus, the height of a MoS<sub>2</sub> can be estimated from the EQ mode in the measured scattering spectrum. The evolution of the integration of  $E^4$  over the volume of a MoS<sub>2</sub> nanoparticle with increasing height, which reflects the SHG efficiency, is presented in Fig. S4b. Here, we consider only symmetric modes (ED and MD modes). It is found that the SHG efficiency exhibits a strong dependence on the height of the MoS<sub>2</sub> nanoparticle.

In Fig. S4c, we show the scattering spectra calculated for MoS<sub>2</sub> nanoparticles with the same height ( $h = 170$  nm) and different lengths ( $l = 130$ – $210$  nm). It can be seen that the scattering cross-sections of all modes increased with increasing length, especially the ED mode. The SHG efficiencies calculated for the ED and MD modes with increasing height are presented in Fig. S4d. As the length increases, the SHG efficiency also increases rapidly.

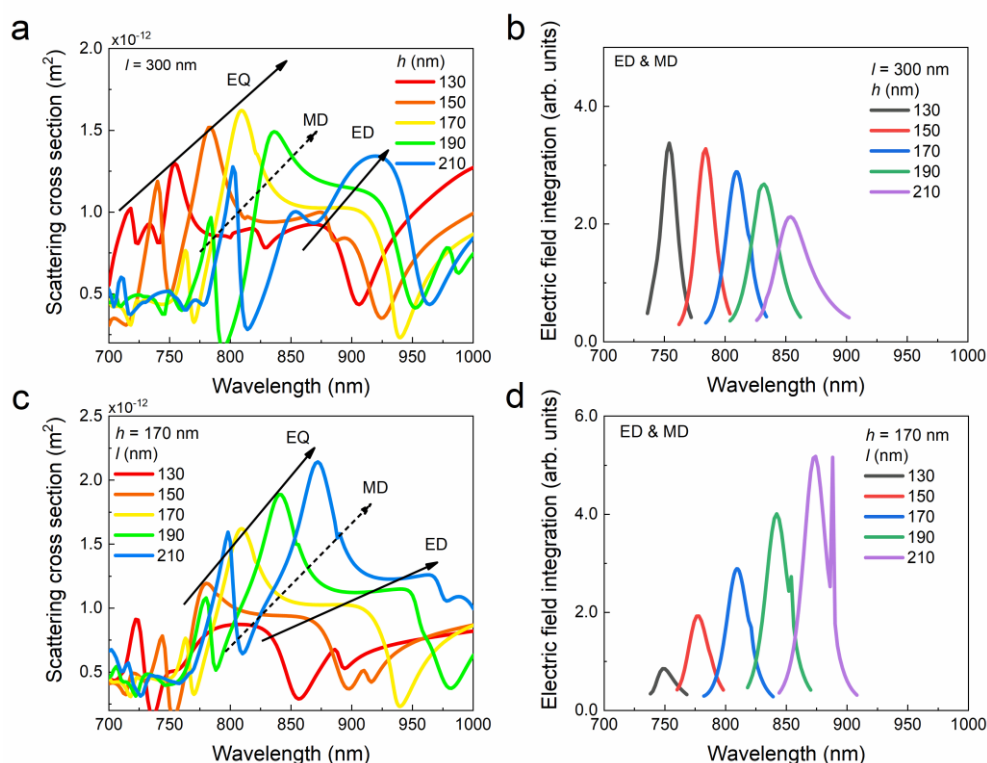


Figure S4 (a) Scattering spectra calculated for MoS<sub>2</sub> nanoparticles with the same length and different heights. (b) The evolution of the SHG efficiency of a MoS<sub>2</sub> nanoparticle with increasing height. (c) Scattering spectra calculated for MoS<sub>2</sub> nanoparticles with the same height and different lengths. (d) Evolution of the SHG efficiency of a MoS<sub>2</sub> nanoparticle with increasing length.

## Note 5 CCD images of the SHG

The emission pattern of the SHG from a MoS<sub>2</sub> nanoparticle exhibits a dependence on the excitation wavelength (i.e., the wavelength of the fundamental wave). In Fig. S5, we show the

emission patterns of the SHG observed at different excitation wavelengths, which are recorded by using a charge coupled device (CCD).

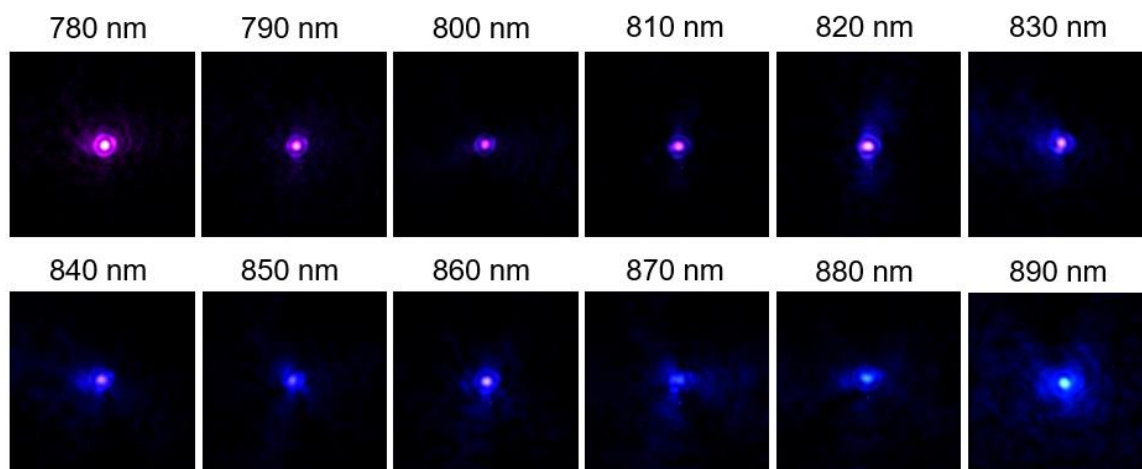


Figure S5 CCD images of the SHG observed at different excitation wavelengths.

#### Note 6 Optical mode with suppressed SHG

In Fig. S6a, we show the scattering spectrum measured for a MoS<sub>2</sub> nanoparticle. Apparently, a scattering peak appears at ~800 nm. In Fig. S6b, we present the SHG spectra measured at different excitation wavelengths. It is noticed that the minimum SHG is observed at ~800 nm. It implies that the optical mode at ~800 nm is the one with suppressed SHG.

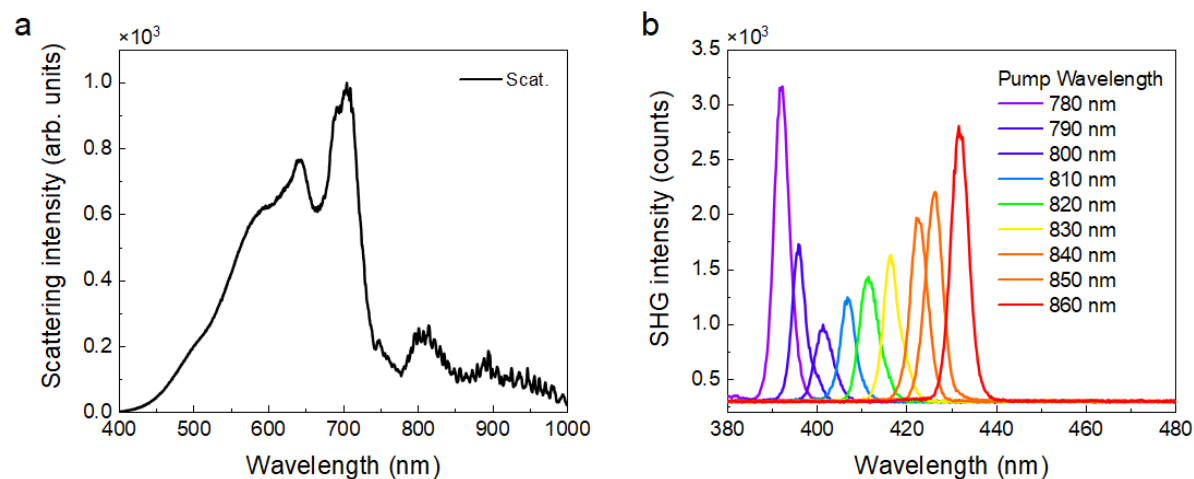


Figure S6 (a) Scattering spectrum measured for a MoS<sub>2</sub> nanoparticle. (b) SHG spectra measured at different excitation wavelengths for the MoS<sub>2</sub> nanoparticle shown in (a).

#### Note 7 Optical mode with enhanced SHG

In Fig. S7a, we show the scattering spectrum measured for a MoS<sub>2</sub> nanoparticle. Apparently, a scattering peak appears at ~830 nm. In Fig. S7b and S7c, we present the SHG spectra measured at different excitation wavelengths by using a 60 $\times$  and a 100 $\times$  objective, respectively. Except the

excitation and collection efficiencies, it is noticed that the maximum SHG is observed at  $\sim 830$  nm. It implies that the optical mode at  $\sim 830$  nm is the one with enhanced SHG.

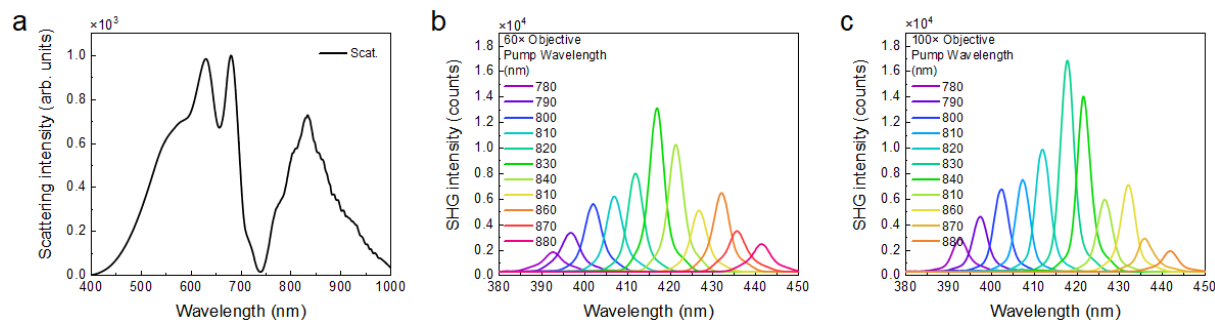


Figure S7 (a) Scattering spectrum measured for a MoS<sub>2</sub> nanoparticle. (b) and (c) SHG spectra measured at different excitation wavelengths for the MoS<sub>2</sub> nanoparticle shown in (a) by using a 60 $\times$  and a 100 $\times$  objective, respectively.

#### Note 8 Emission pattern of the SHG

The three-dimensional (3D) emission pattern of the SHG of a MoS<sub>2</sub> nanoparticle can be obtained by using a laser scanning confocal microscope. In Fig. S8a, we show the 3D emission pattern of the SHG observed for the MoS<sub>2</sub> nanoparticle shown in Figure 3a-c at the optical mode with suppressed SHG. In this case, the suppressed SHG appearing at the center is not revealed due to the existence of the surface nonlinearity. Actually, the nanohole originating from the vanishing of the bulk nonlinearity is hidden inside. In Fig. S8b we show the 3D emission pattern of the SHG for the MoS<sub>2</sub> nanoparticle shown in Figure 3d-f at the optical mode with enhanced SHG.

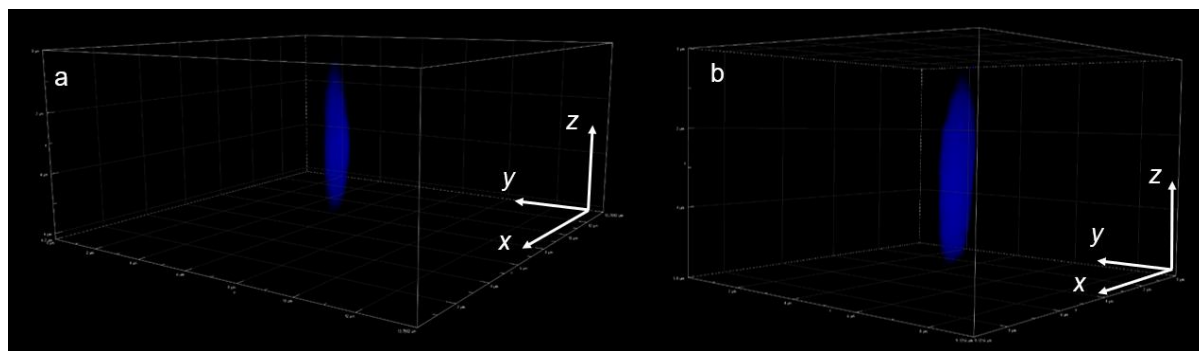


Figure S8 3D emission patterns of the SHG at the optical modes with suppressed (a) and enhanced (b) SHG.

#### Note 9 Selecting MoS<sub>2</sub> nanoparticles with suppressed SHG by using laser scanning confocal microscopy

In practice, we can identify MoS<sub>2</sub> nanoparticles with suppressed SHG by using a laser scanning confocal microscope. A typical example is shown in Fig. S9 where the SHG emission patterns obtained for MoS<sub>2</sub> nanoparticles distributed on a substrate are presented. The MoS<sub>2</sub> nanoparticle exhibit a suppressed SHG is enclosed by a square. One can observe a nanohole at the center of the emission pattern.

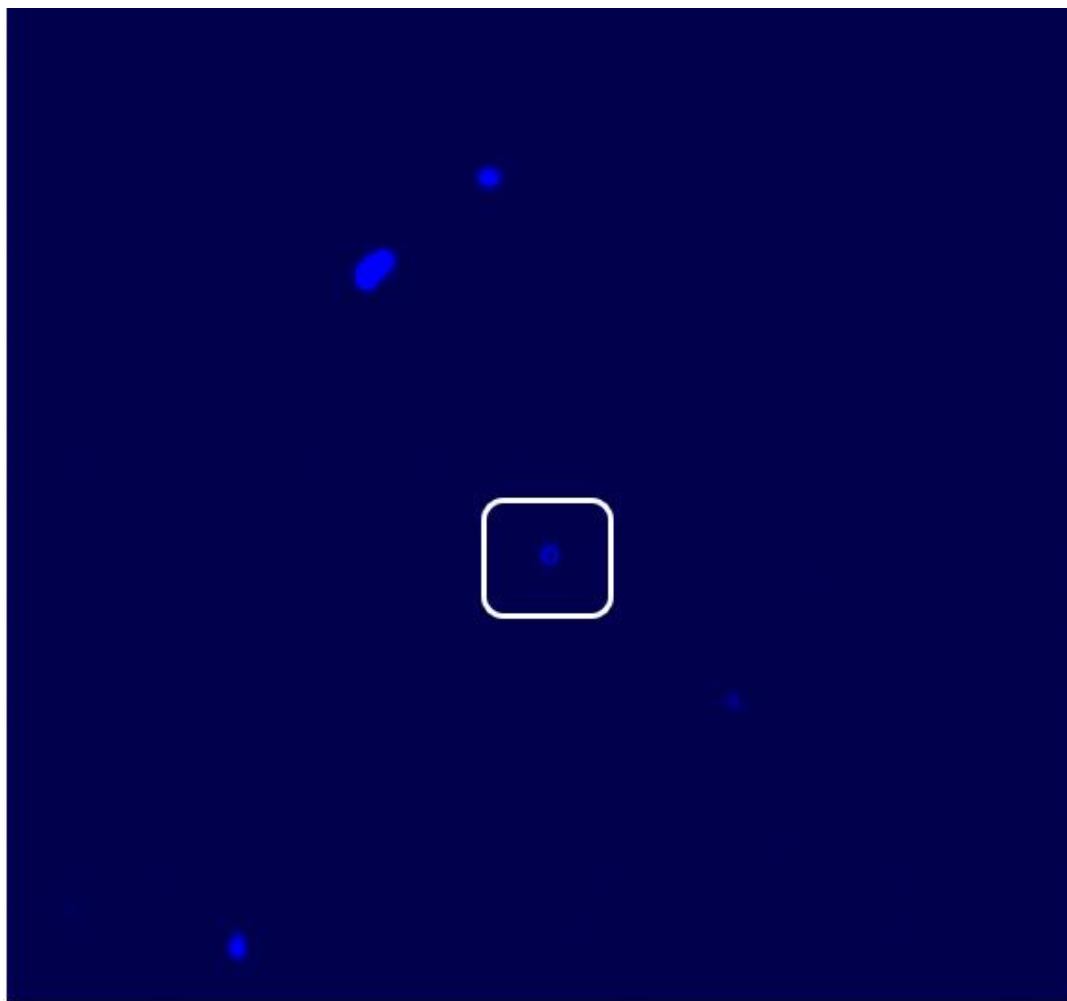


Figure S9 SHG emission patterns obtained for MoS<sub>2</sub> nanoparticles distributed on a substrate by using a laser scanning confocal microscope.

Note 10 MoS<sub>2</sub> monolayer attached on an ITO substrate

In Fig. S10, we show a MoS<sub>2</sub> monolayer attached on an ITO substrate. It was used as a reference sample for the SHG characterization. The MoS<sub>2</sub> monolayer was grown by chemical vapor deposition (CVD) and transferred to the ITO substrate.



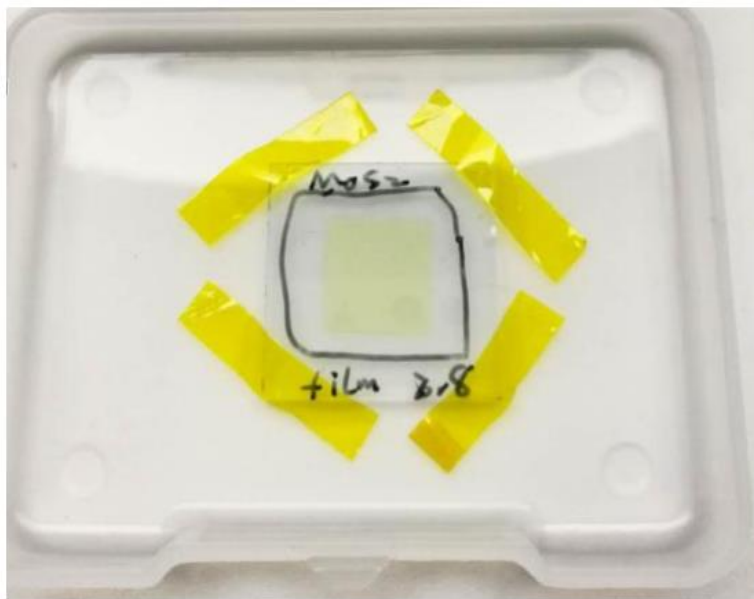


Figure S10 MoS<sub>2</sub> monolayer attached on an ITO substrate used as reference sample.

#### Note 11 Nonlinear optical responses of MoS<sub>2</sub> nanodisks

The MoS<sub>2</sub> monolayer was grown by chemical vapor deposition (CVD) and transferred to the ITO substrate. In our experiments, we investigated the nonlinear optical responses of hexagonal-prism-like MoS<sub>2</sub> nanoparticles selected from MoS<sub>2</sub> powder. In most cases, their shapes deviate from perfect hexagonal prisms. Thus, it is highly desirable to examine the nonlinear optical response of MoS<sub>2</sub> nanoparticles with regular shapes. For this reason, we fabricated MoS<sub>2</sub> nanodisks from a MoS<sub>2</sub> film grown by chemical vapor deposition on a sapphire substrate with the combination of electron beam lithography and reactive ion etching. The SEM images of MoS<sub>2</sub> nanodisks with different diameters are shown in Figs. S11a and S11b.

We measured the scattering spectra of MoS<sub>2</sub> nanodisks with different diameters, as shown in Fig. S11c. Unfortunately, we did not observe the scattering dips corresponding to the exciton resonances of MoS<sub>2</sub> and any optical resonances in the near infrared spectrum. Also, we did not detect any nonlinear optical signals when such MoS<sub>2</sub> are excited by using femtosecond laser pulses.

In order to find out the physical origin for this abnormal behavior, we measured the X-ray diffraction (XRD) spectrum for the MoS<sub>2</sub> film (red curve) used to fabricate the MoS<sub>2</sub> nanoparticles, as shown in Fig. S11d. The X-ray diffraction spectrum of a hexagonal-prism-like MoS<sub>2</sub> nanoparticle (black curve) is also provided for comparison. It was found that most peaks appearing in the spectrum of the MoS<sub>2</sub> nanoparticle are missing in the spectrum of the MoS<sub>2</sub> film. By comparing the X-ray diffraction spectra reported in literature, it was confirmed that MoS<sub>2</sub> nanoparticles are single crystalline while MoS<sub>2</sub> nanodisks are polycrystalline. This is the reason why both exciton resonances and optical resonances are not observed in MoS<sub>2</sub> nanodisks.

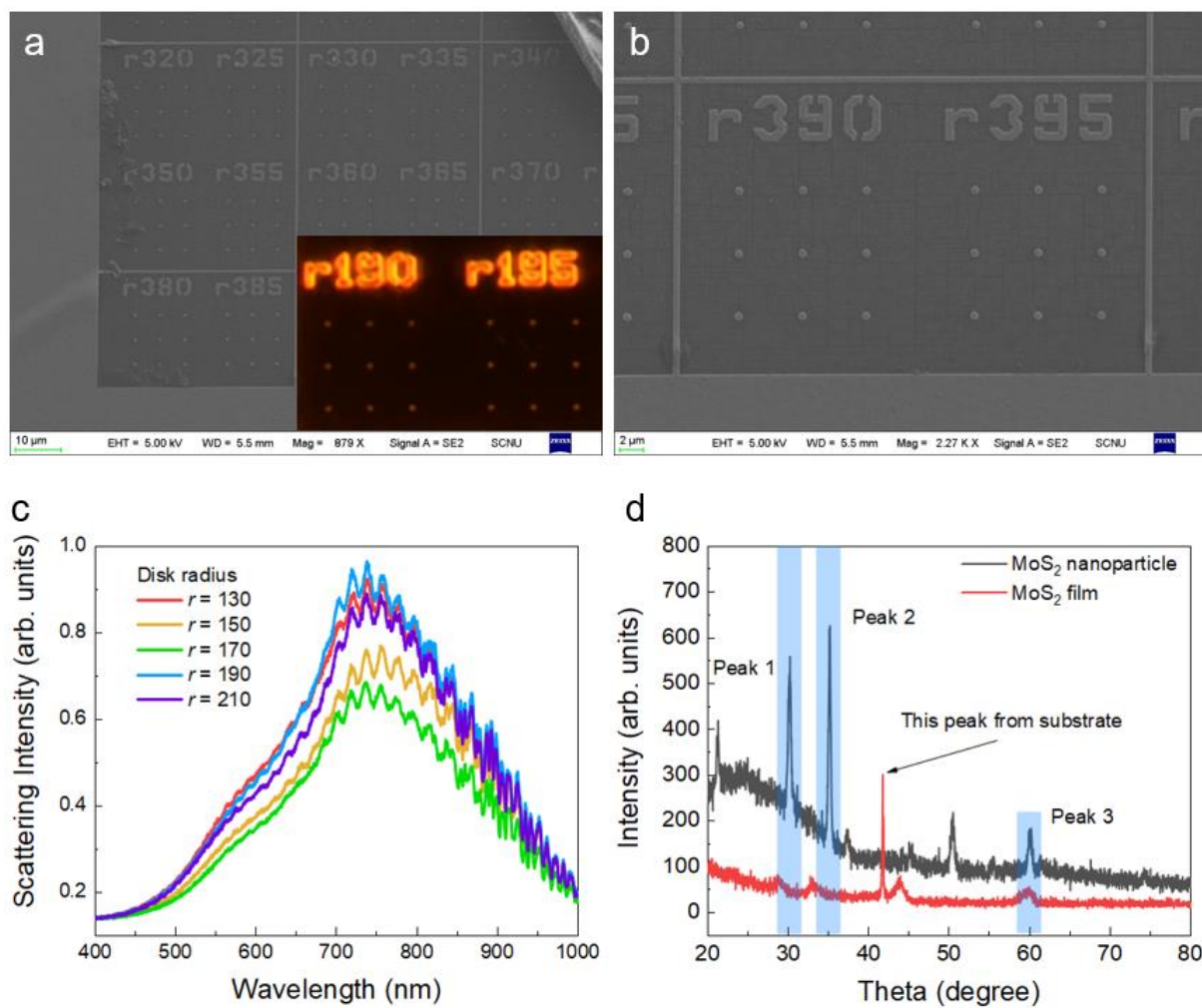


Figure S11 (a) and (b) SEM images of MoS<sub>2</sub> nanodisks with diameters fabricated on a sapphire substrate. (c) Scattering spectra measured for MoS<sub>2</sub> nanodisks with different diameters. (d) X-ray diffraction spectrum measured for the MoS<sub>2</sub> film (red curve) used to fabricate MoS<sub>2</sub> nanodisks. The X-ray diffraction spectrum of a MoS<sub>2</sub> nanoparticle (black curve) is also provided for reference.